Supplementary Material

Bayesian Divergence-Time Estimation with Genome-Wide SNP Data of Sea Catfishes (Ariidae) Supports Miocene Closure of the Panamanian Isthmus

Madlen Stange,[1,2†] Marcelo R. Sánchez-Villagra,[1] Walter Salzburger[2,3] and Michael Matschiner[2,3†]

Addresses:

[1]Department of Palaeontology and Museum, University of Zurich, Karl-Schmid-Strasse 4, 8006 Zurich, Switzerland

[2]Zoological Institute, University of Basel, 4051 Basel, Switzerland

[3]Centre for Ecological and Evolutionary Synthesis (CEES), Department of Biosciences, University of Oslo, 0316 Oslo, Norway

[†]Corresponding author: E-mail: madlen.stange@pim.uzh.ch, michaelmatschiner@mac.com

1 Supplementary Text

Supplementary Text S1: Parameter operators used in divergence-time estimation with SNAPP.
Clock rate: As a single operator on the clock rate, the standard scale operator implemented in SNAPP is used (described in Drummond et al. 2002).
Speciation rate: Like for the clock rate, a scale operator is used also for the speciation rate.
Population sizes: In order to link the Θ values of all branches, all operators on Θ are replaced with a single scale operator that changes all Θ values by the exact same scale value whenever its proposals are accepted.
Tree topology: For analyses of simulated data sets, we fixed the species-tree topology to the true species tree by excluding operators on the species tree. In contrast, our analyses of empirical data employed SNAPP's "NodeSwapper" operator to propose changes to the species-tree topology. When producing XML input files for SNAPP with our script "snapp_prep.rb", the NodeSwapper operator is included by default, but can be turned off with option "-w/--weight = 0".

Supplementary Text S2: Computational requirements of divergence-time estimation with SNAPP.
SNAPP analyses were conducted on the Abel computing cluster provided by the University of Oslo, using four threads on dual eight-core Intel Xeon E5-2670 (Sandy Bridge-EP) CPUs running at 2.6 GHz. We performed between 400 000 and 18.4 million Markov-chain Monte Carlo (MCMC) iterations per SNAPP analysis (Supplementary Table S2). For each SNAPP analysis of simulated data sets, we recorded i) the time required per MCMC iteration, ii) the number of iterations required for convergence (ESS $\geq$ 200) of all parameters, and iii) the time required for convergence as the product of i) and ii).

The computational time required per MCMC iteration increased with the number of SNPs analyzed, the population size used in simulations, and the number of diploid indidivuals sampled per species (Supplementary Figure S4, Supplementary Table S2). The effect of the number of SNPs was less strong than that of the number of unique site patterns in each data set. The data sets of 300, 1 000, and 3 000 SNPs included 64 to 100 (mean: 81.8), 112 to 166 (mean: 138.0), and 183 to 280 (mean: 232.4) unique site patterns, respectively, and therefore showed a less-than-linear increase of the number of unique sites with the number of SNPs. With most settings, the time per iteration was on the order of 0.15-0.50 seconds. The exeptions to this were analyses with different sample sizes in experiment 3; these required on average only 0.05 seconds with a sample size of 1 diploid individual per species, or close to 2 seconds with a sample size of 4 individuals (Supplementary Table S2).

The number of MCMC iterations required for convergence (all ESS values $\geq$ 200) increased with the number of SNPs when constraints were placed on the root node. This relationship was inversed when younger age constraints were used, presumably due to narrower peaks in the probability surface with larger SNP numbers. The number of MCMC iterations required also increased with larger simulated population sizes; however, the sample size had little influence on it.

As a result, the computational time required for convergence was driven by a combination of

the size of the data set, the placement of the node-age constraint, the population size, and the number of sampled individuals. The latter parameter had the strongest impact on computational time: With a sample size of 1 diploid individual, analyses converged on average after 4.5 hours, but required over 200 hours on average with a sample size of 4 individuals (Supplementary Table S2). The fastest analysis (which used a sample size of 1) converged after 4.0 hours, while the slowest analysis (with a sample size of 4) took over 106 days to converge.

The observation that the number of unique site patterns determines computational requirements more directly than the number of SNPs suggests that further extensions to the SNP data may have relatively little impact on these requirements when many of the site patterns included in these extensions are already present in the data set. Nevertheless, the addition of these SNPs would further improve the precision of divergence-time estimates, which implies that even analyses with extremely large numbers of SNPs may be worthwhile. However, how rapidly the set of unique site patterns approaches saturation likely varies among data sets and will depend on factors such as the number of species, the number of specimens per species, and the proportion of missing data.

2 Supplementary Figures

Supplementary Figure S1: Exemplary species tree and gene trees.
a) Visual representation of one out of the 100 simulated species trees. b-d) Cloudograms of gene trees simulated for the species tree shown in a) with a population size of 25 000 (b), 100 000 (c), and 400 000 (d) diploid individuals. The generation time used in simulations was 5 years.

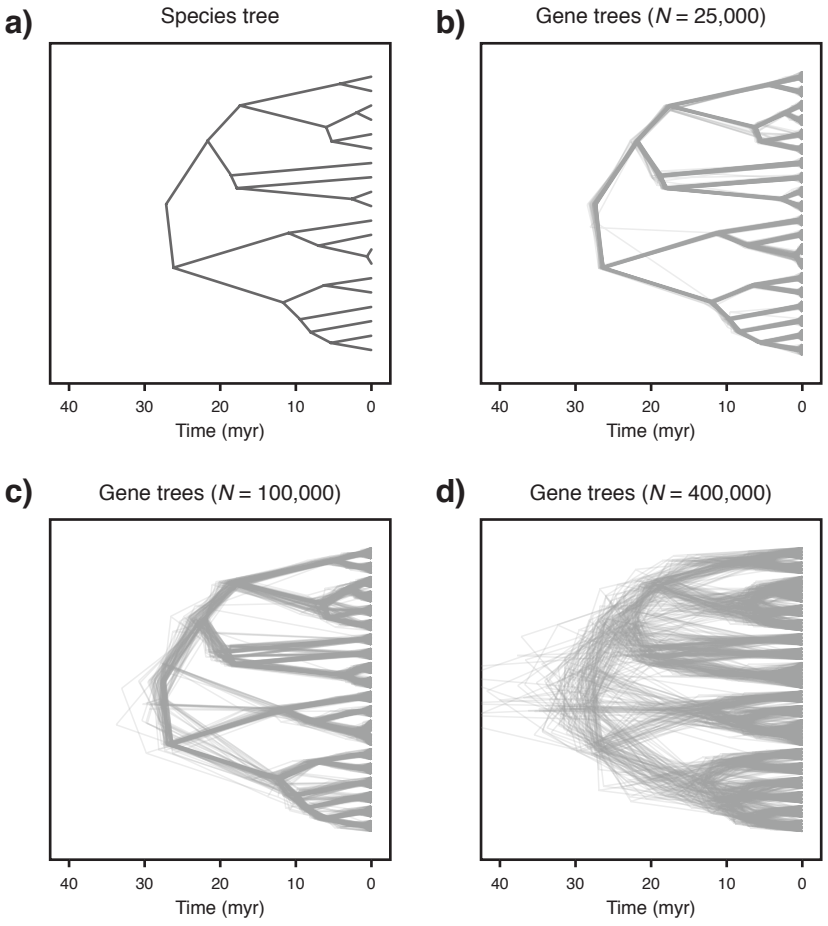

Supplementary Figure S2: Comparison of true and estimated node ages with different simulated population sizes (experiment 2).
In experiment 2, we compared node-age estimates obtained with data sets that were simulated with different population sizes, these were $N = 25\,000$, $N = 100\,000$, and $N = 400\,000$ diploid individuals. All results are based on 100 simulated species trees with 20 extant species, 2 diploid individuals sampled from each species, and 1 000 SNPs analyzed per individual. Node ages were estimated with an age constraint on the root node in all analyses of experiment 2. Only unconstrained nodes are shown. The plot shown for a population size of $N = 25\,000$ is identical to the one in the left column of Figure 2, for results based on ascertainment-bias correction.

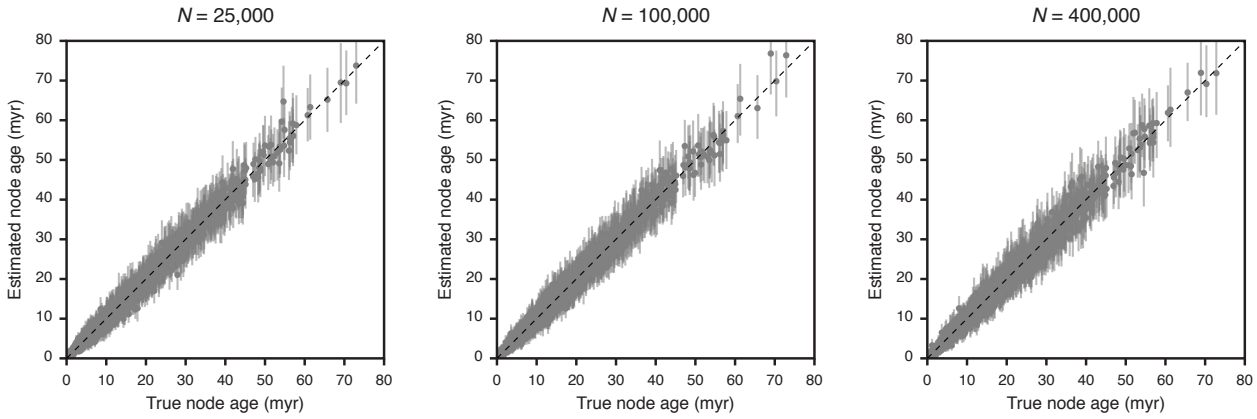

Supplementary Figure S3: Computational time requirements of SNAPP analyses.
The time required per MCMC iteration, the number of iterations required for convergence (ESS values for all parameters ≥ 200), and the resulting time required for convergence are compared for analyses of experiments 1-3. a) Computational time requirements of analyses conducted for experiment 1, with data sets comprising 300, 1 000, and 3 000 SNPs, and with age constraints on either the root node (dark gray) or a younger node (light gray). Population sizes and sample sizes did not vary in experiment 1: the population size was set to $N = 25\,000$ diploid individuals, of which 2 diploid individuals were sampled (see Table 1 and Supplementary Table S2). b) Time requirements of analyses conducted for experiment 2, for data sets simulated with population sizes of $N = 25\,000$, $N = 100\,000$, and $N = 400\,000$ diploid individuals. All analyses conducted in experiment 2 were based on a sample size of 2 diploid individuals, a data-set size of 1 000 SNPs, and an age constraint on the root node. Thus, the computational requirements shown in b) for a population size of 25 000 diploid individuals are identical to those reported in a) for a data-set size of 1 000 SNPs and age constraints on the root, and are included here for completeness. c) Time requirements of analyses conducted for experiment 3, in which sample sizes of 1, 2, or 4 diploid individuals per species were used. All data sets used in experiment 3 were simulated with a population size of $N = 25\,000$ diploid individuals. These data sets invariably included 1 000 SNPs and were analyzed with an age constraint on the root node. The requirements shown in c) for a sample size of 2 diploid individuals are identical to those shown in b) for a population size of $N = 25\,000$.

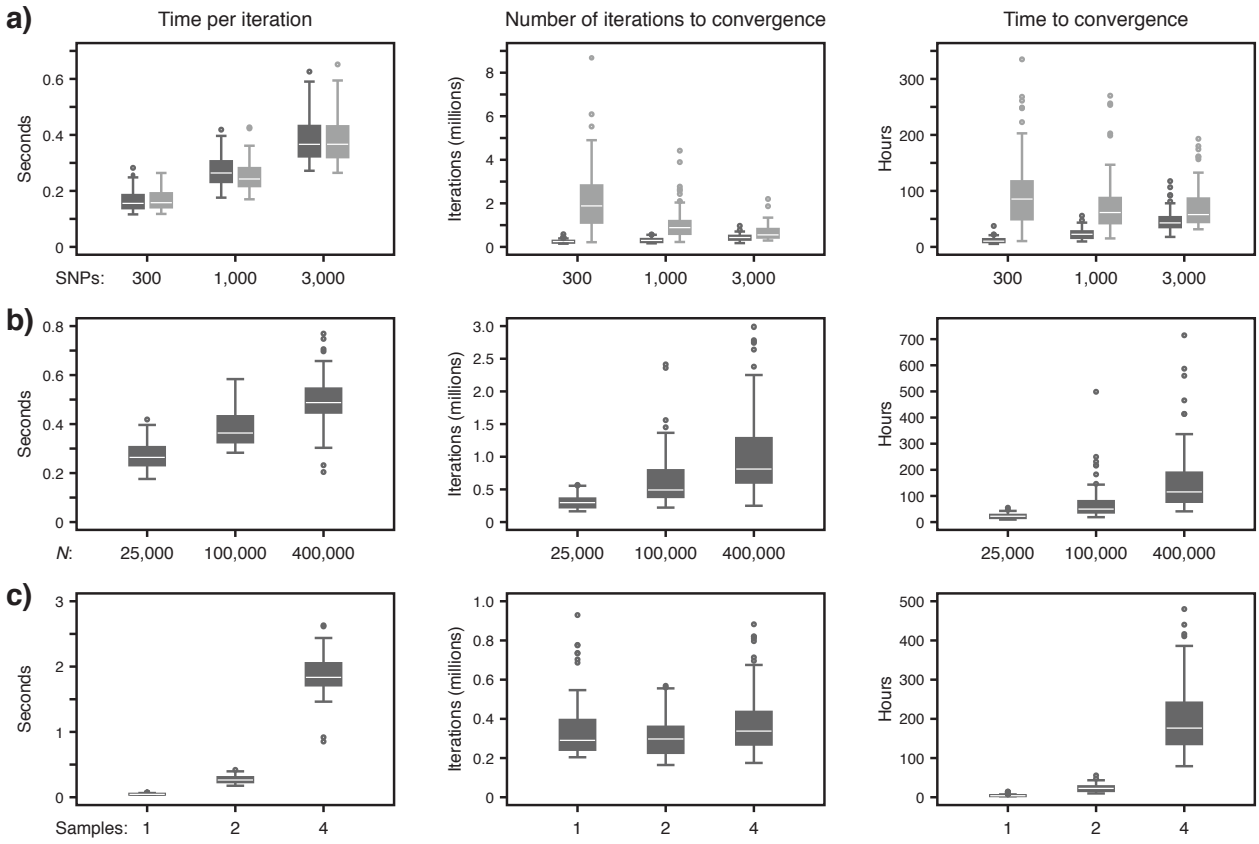

Supplementary Figure S4: Comparison of true and estimated node ages with varying sample sizes (experiment 3).
In experiment 3, we compared node-age estimates obtained with different sample sizes; per species we sampled 1, 2, or 4 diploid individuals. All results are based on 100 simulated species trees with 20 extant species, a population size of $N = 25\,000$ diploid individuals, and 1 000 SNPs analyzed per individual. Node ages were estimated with an age constraint on the root node in all analyses of experiment 3. Only unconstrained nodes are shown. The plot shown for a sample size of 2 is identical to the one in the left column of Figure 2, for results based on ascertainment-bias correction.

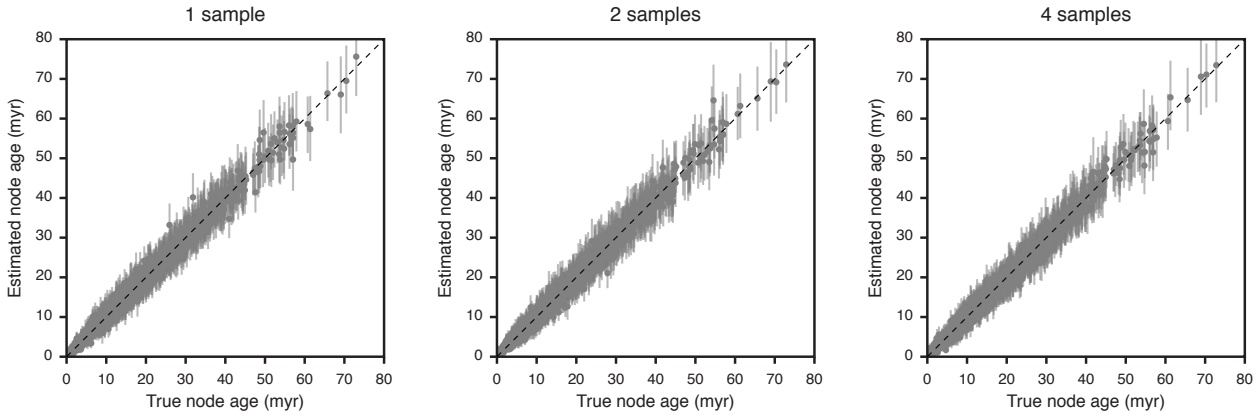

Supplementary Figure S5: Maximum-clade-credibilty tree of Neotropical army ants based on the MSC model.
Node heights correspond to mean node-age estimates. Node ids are provided to allow comparison to node support and age estimates given in Supplementary Table S3. Colors indicates genera: *Eciton*, blue-green; *Nomamyrmex*, green; *Labidus*, yellow; *Cheliomyrmex*, light brown; *Neivamyrmex*, dark brown. CA, Central America; SA, South America.

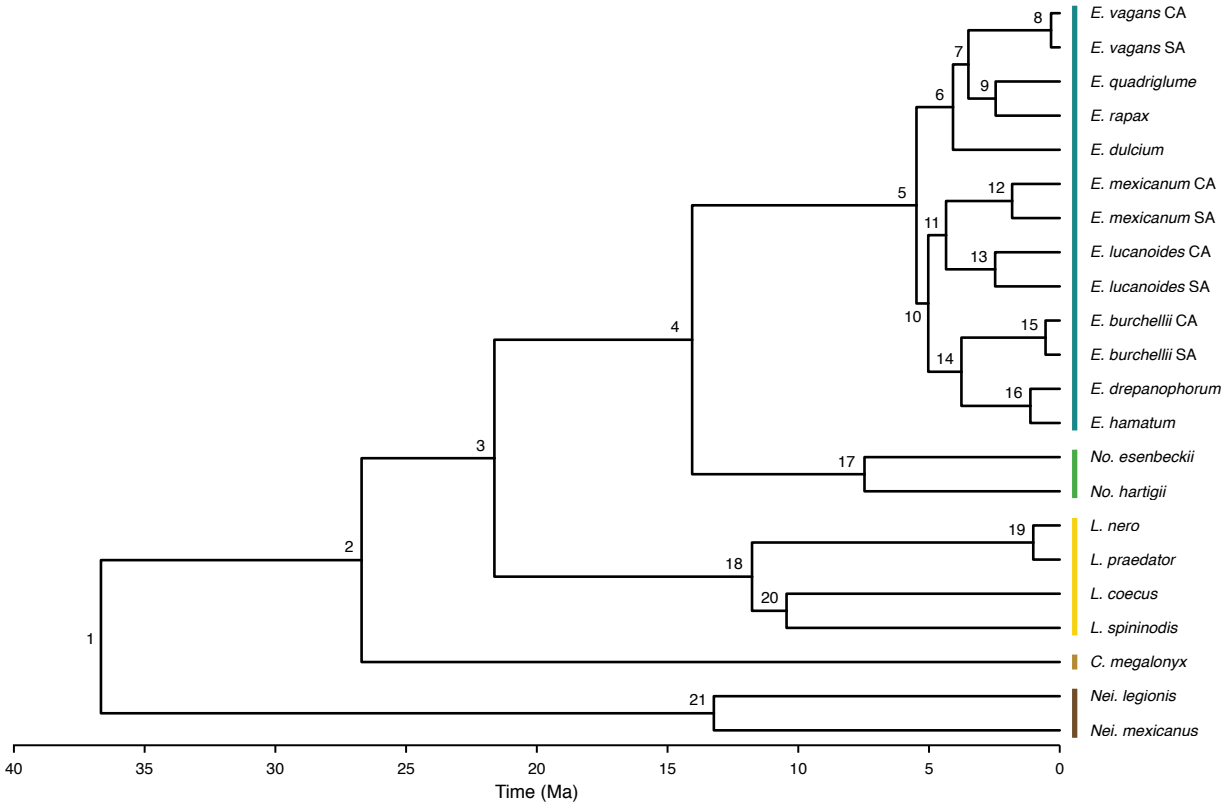

Supplementary Figure S6: Maximum-clade-credibilty tree of Neotropical army ants based on concatenation.
Node heights correspond to mean node-age estimates. Node ids are provided to allow comparison to node support and age estimates given in Supplementary Table S4. Colors indicates genera as in Supplementary Figure S5: *Eciton*, blue-green; *Nomamyrmex*, green; *Labidus*, yellow; *Cheliomyrmex*, light brown; *Neivamyrmex*, dark brown. CA, Central America; SA, South America.

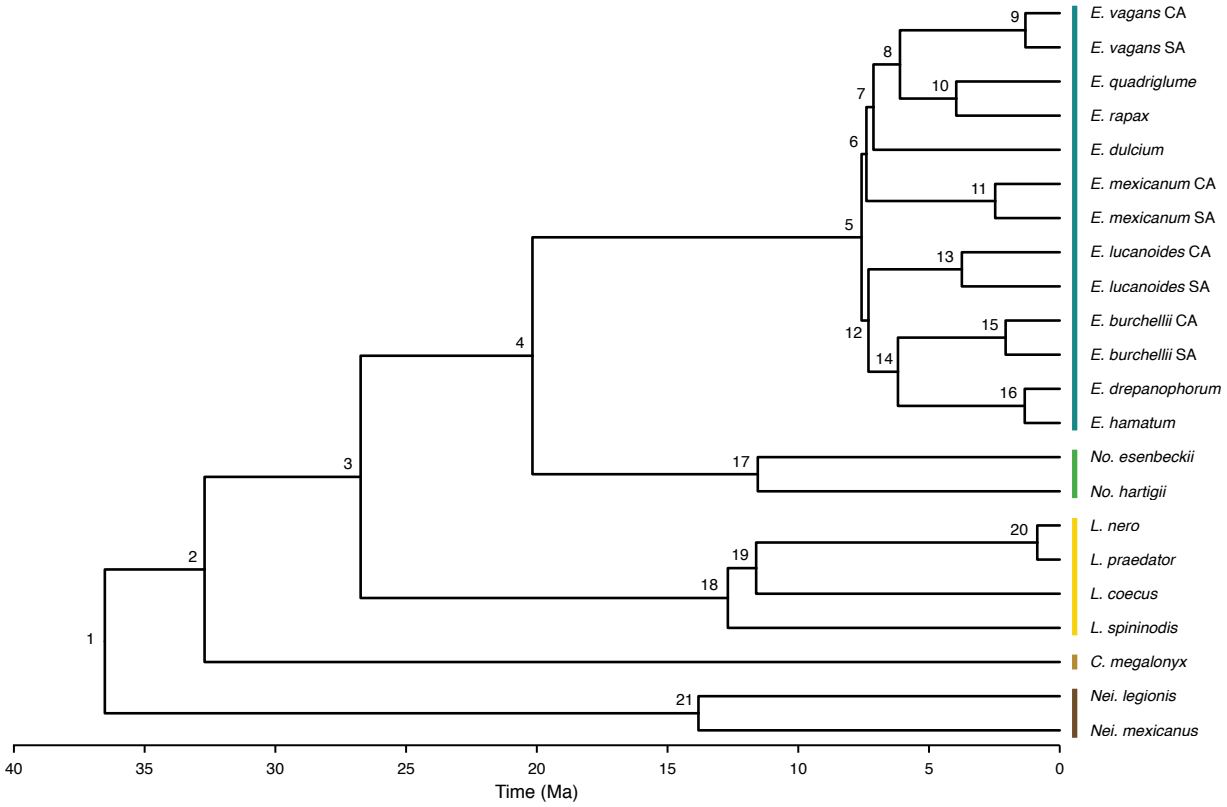

Supplementary Figure S7: Maximum-clade-credibilty tree of Neotropical sea catfishes based on the MSC model.

To allow the reconstruction of ancestral geographic distributions taking into account fossil localities, eight fossil taxa were added a posteriori according to their taxonomic assignment: *Cathorops goeldii* (Aguilera et al. 2013) was attached to the stem branch of the genus *Cathorops* with a tip age of 20.4 Ma, reflecting the minimum age of the Pirabas Formation from which this fossil was described. Similarly, *Notarius* sp. and *Bagre protocaribbeanus* from the same formation (Aguilera et al. 2013) were added to the stem branches of the genera *Notarius* and *Bagre*, respectively. In addition, *Bagre protocaribbeanus* from the Venezuelan Cantaure Formation was added as the sister of the older *B. protocaribbeanus* fossil from the Pirabas Formation, with a tip age of 16.0 Ma. Finally, fossil representatives of the species *Sciades dowii*, *Sciades herzbergii*, *Bagre marinus*, and *Notarius quadriscutis* were added as sister branches of these extant taxa, with a tip age corresponding to the minimum age of the Urumaco Formation, 5.3 Ma (see Supplementary Table S6). Node heights correspond to mean node-age estimates. Node ids are provided to allow comparison to node support, age estimates, and reconstructed ancestral geography given in Supplementary Table S7. Colors indicates genera as in Figure 4 and in Stange et al. (2016): *Ariopsis*, red; *Sciades*, purple; *Bagre*, blue; *Notarius*, green; *Cathorops*, orange.

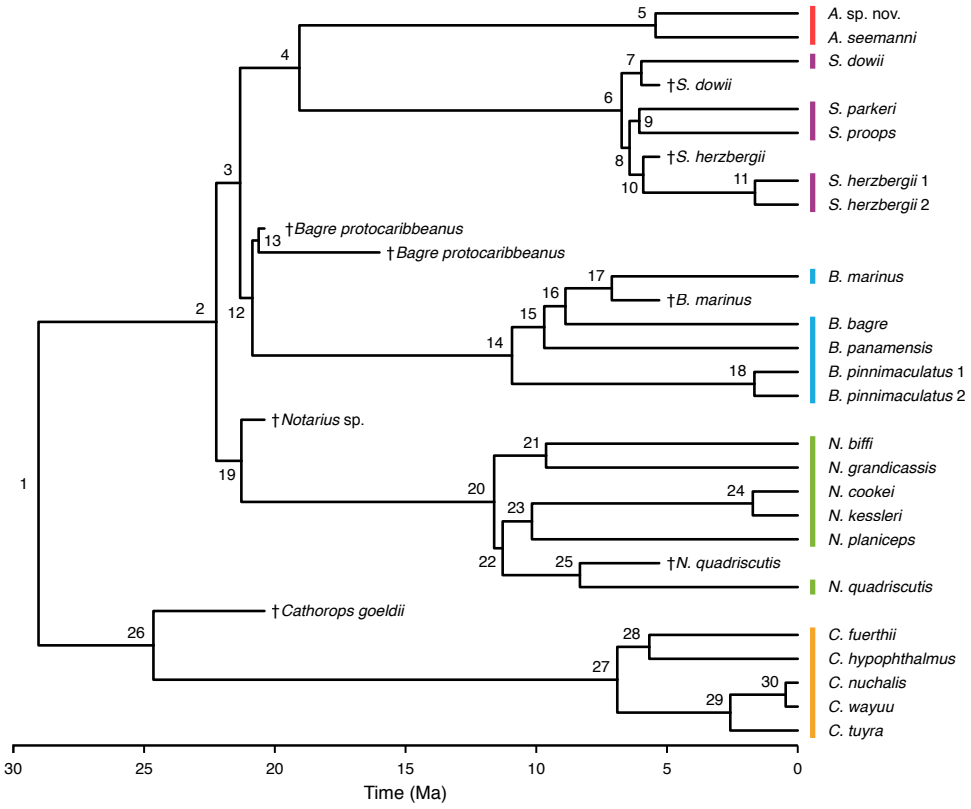

3 Supplementary Tables

Supplementary Table S1: Studies using SNAPP, published before November 2017.

Study	Analysis type	Groups	Individuals	Loci
Afonso Silva et al. (2017)	BFD*	2-4	20	2 163 SNPs
Ahrens et al. (2017)	phylogeny	17	97	874 SNPs
Alter et al. (2017)	phylogeny	23	53	11 459-37 826 SNPs
Anderson et al. (2017)	phylogeny	11	67	983-1 335 SNPs
Battey and Klicka (2017)	phylogeny, BFD*	4-6	40	938-7 799 SNPs
Beddows et al. (2017)	phylogeny	71	71	1 250 SNPs
Bell et al. (2015)	phylogeny	4	21	467 SNPs
Blanca et al. (2015)	phylogeny	16	16	2 313 SNPs
Boucher et al. (2016)	BFD*	1-4	90	1 449-1 665 SNPs
Bryant et al. (2012)	phylogeny	6	69	1 997 AFLP
Bryson et al. (2016)	phylogeny	9	54	312 SNPs
Burns and Tsurusaki (2016)	phylogeny	5	20	226 SNPs
Card et al. (2016)	BFD*	2-3	33	1 686 SNPs
Chan et al. (2017)	phylogeny, BFD*	2-5	117	4 744-17 123 SNPs
Chifman and Kubatko (2014)	phylogeny	10	20	1 027 026 SNPs
Clucas et al. (2016)	phylogeny	4	8	2 626-2 668 SNPs
Cooper and Uy (2017)	phylogeny	4	12	7 000 SNPs
DaCosta and Sorenson (2016)	phylogeny	10-15	10-15	2 856-3 098 SNPs
De Maio et al. (2015a)	phylogeny	4-8	4-80	3-1 000 genes
Demos et al. (2015)	phylogeny	6-7	28-31	52 580-56 194 SNPs
Dupuis et al. (2017)	phylogeny	8	8	5 704 SNPs
Foote and Morin (2016)	phylogeny	5	43	1 346 SNPs
Ford et al. (2015)	phylogeny	11	44	1 266 SNPs
Fraser et al. (2016)	BFD*	3	73	75 712 SNPs
Giarla and Esselstyn (2015)	phylogeny	9-19	19	1 170 SNPs
Gohli et al. (2014)	phylogeny	10	59	166-2 000 SNPs
Gottscho et al. (2017)	BFD*	2-6	64	468 SNPs
Gratton et al. (2016)	BFD*	4-6	46	2 039 SNPs
Hamlin and Arnold (2014)	phylogeny	6-12	43-67	560-1 140 SNPs
Harrington et al. (2017)	phylogeny	3	35	718 SNPs
Harris et al. (2017)	phylogeny	16	64	1 467 SNPs
Harvey and Brumfield (2015)	phylogeny	5-8	72	3 379 SNPs
Herrera and Shank (2016)	phylogeny, BFD*	3-24	31	1 203 SNPs
Hulsey et al. (2017)	phylogeny	34	34	13 698 SNPs
Johansson et al. (2017)	phylogeny	9	78	1 674 SNPs
Kautt et al. (2016)	phylogeny	7	28	1 290-1 772 SNPs
Kordbacheh et al. (2017)	phylogeny	62	62	10 AFLPs
Lambert et al. (2013)	phylogeny	4	138	821 AFLPs
Leaché et al. (2014)	BFD*	2-5	46	129-1 087 SNPs
Li et al. (2015)	phylogeny, BFD*	4-10	10	1 041 SNPs
Lischer et al. (2014)	phylogeny	4	15	1 552 SNPs
Lozier et al. (2016)	phylogeny	5	41	1 568 SNPs
MacGuigan et al. (2017)	phylogeny, BFD*	2-13	41-82	534-836 AFLPs
MacLeod et al. (2015)	phylogeny	12	33	6 257 SNPs
Malinsky et al. (2017)	phylogeny	12	12	48 922 SNPs

BFD*, Bayes Factor delimitation with genomic data (Leaché et al. 2014)

Supplementary Table S1 (continued):

Study	Analysis type	Groups	Individuals	Loci
Manthey et al. (2015)	phylogeny	8	41	13 421 SNPs
Manthey et al. (2016)	phylogeny	16	30	605-1 128 SNPs
Mason and Taylor (2015)	BFD*	2-4	20	35-1 587 SNPs
McCormack et al. (2015)	phylogeny	26	26	1 388 SNPs
Meier et al. (2017)	phylogeny	16	31	1 817 SNPs
Meik et al. (2015)	phylogeny	5	26	2 409 SNPs
Morin et al. (2015)	phylogeny	12	113	42 SNPs
Mrinalini et al. (2015)	BFD*	2-4	50	298 AFLPs
Nater et al. (2015)	phylogeny	4	48	16 000 SNPs
Ng et al. (2017)	phylogeny	4	18	6 650 SNPs
Nicotra et al. (2016)	phylogeny	8	23	463 SNPs
Nieto-Montes de Oca et al. (2017)	BFD*	1-4	50	401-430 SNPs
Ogilvie et al. (2016)	phylogeny	8-12	11-45	791-5 907 SNPs
Olšavská et al. (2016)	phylogeny	14	120	442 AFLPs
Oswald et al. (2016)	BFD*	2-3	13	14 285 SNPs
Papadopoulou and Knowles (2017)	phylogeny	7-13	21-39	1 155-1 896 SNPs
Paun et al. (2016)	phylogeny	26	79	1 506 SNPs
Portik et al. (2017)	phylogeny	6	25	1 520 SNPs
Potter et al. (2016)	phylogeny, BFD*	3-5	8-14	2 084 SNPs
Razkin et al. (2016)	phylogeny, BFD*	7-10	25	368-875 SNPs
Rheindt et al. (2014)	phylogeny	4-5	12	947-954 SNPs
Rittmeyer and Austin (2015)	BFD*	2-3	12	941-1 973 SNPs
Rodríguez et al. (2017)	phylogeny	6	11	3 586 SNPs
Schield et al. (2017)	phylogeny, BFD*	2-3	75	7 031 SNPs
Schmidt-Lebuhn et al. (2017)	phylogeny	8	24	500 SNPs
Sovic et al. (2016)	phylogeny, BFD*	2-5	12-15	1 099 SNPs
Stervander et al. (2016)	phylogeny	6-7	12	1 590-26 629 SNPs
Stervander et al. (2015)	phylogeny	16	16	3 421 SNPs
Stetter and Schmid (2017)	phylogeny	35	94	1 605 SNPs
Streicher et al. (2014)	phylogeny	9	39	353 SNPs
Takahashi et al. (2016)	phylogeny	10	60	390 AFLPs
Takahashi et al. (2015)	phylogeny	8	90	522 AFLPs
Tremetsberger et al. (2016)	phylogeny	4	36	207 AFLPs
Wagner et al. (2017)	BFD*	2-6	53	349 AFLPs
Winger et al. (2015)	phylogeny	6	14	1 767 SNPs
Yoder et al. (2016)	phylogeny	6	29	3 986-4 613 SNPs
Younger et al. (2017)	phylogeny	8	110	3 221-3 237 SNPs
Yuan et al. (2016)	phylogeny	6	6	2 921 SNPs
Zarza et al. (2016)	phylogeny	24	24	2 501 SNPs

BFD*, Bayes Factor delimitation with genomic data (Leaché et al. 2014)

Supplementary Table S2: Computational time requirements of SNAPP analyses (experiments 1-3). Mean values are given for the number of iterations and the time required for convergence. Ex. = Experiment.

N	Samples	SNPs	Calibration	Iterations conducted	Time per iteration	Iterations to convergence	Time to convergence	Ex.
25 000	2	300	root node	1 000 000	0.16 secs	254 175	11.7 hrs	1
25 000	2	1 000	root node	1 000 000	0.27 secs	309 455	23.2 hrs	1-3
25 000	2	3 000	root node	1 000 000	0.38 secs	433 035	46.3 hrs	1
25 000	2	300	young node	2 000 000-9 000 000	0.17 secs	2 056 755	94.0 hrs	1
25 000	2	1 000	young node	2 000 000-4 500 000	0.25 secs	1 030 520	72.4 hrs	1
25 000	2	3 000	young node	2 000 000-2 500 000	0.38 secs	662 430	70.2 hrs	1
100 000	2	1 000	root node	500 000-6 974 500	0.39 secs	713 225	76.3 hrs	2
400 000	2	1 000	root node	1 000 000-18 412 500	0.50 secs	1 246 675	172.4 hrs	2
25 000	1	1 000	root node	500 000-1 000 000	0.05 secs	339 285	4.5 hrs	3
25 000	4	1 000	root node	400 000-2 450 000	1.88 secs	413 025	208.7 hrs	3

Supplementary Table S3: Node support and age estimates for the species tree of Neotropical army ants based on the MSC model. Lower and upper boundaries given for age estimates describe 95% HPD intervals. Node ids correspond to those given in Supplementary Figure S5.

		Age estimates (Ma)		
Node	Node support (BPP)	Mean	Upper	Lower
1	1.00	36.67	45.76	27.66
2	1.00	26.70	34.98	19.25
3	1.00	21.62	28.27	15.27
4	1.00	14.06	18.51	9.30
5	1.00	5.48	7.52	3.52
6	0.98	4.08	5.86	2.44
7	0.79	3.49	5.10	2.05
8	1.00	0.33	0.71	0.05
9	0.99	2.45	3.73	1.28
10	0.51	5.03	6.81	3.22
11	0.78	4.35	6.13	2.71
12	1.00	1.82	3.02	0.76
13	1.00	2.47	3.88	1.22
14	1.00	3.76	5.40	2.19
15	1.00	0.54	1.12	0.13
16	1.00	1.12	1.95	0.37
17	1.00	7.47	10.61	4.54
18	1.00	11.77	15.81	7.53
19	1.00	1.01	2.02	0.16
20	0.64	10.45	14.33	6.65
21	1.00	13.23	18.02	8.71

Supplementary Table S4: Node support and age estimates for the species tree of Neotropical army ants based on concatenation. Lower and upper boundaries given for age estimates describe 95% HPD intervals. Node ids correspond to those given in Supplementary Figure S6.

		Age estimates (Ma)		
Node	Node support (BPP)	Mean	Upper	Lower
1	1.00	36.52	45.23	27.38
2	1.00	32.71	40.67	24.70
3	1.00	26.74	33.24	20.19
4	1.00	20.17	25.10	15.25
5	1.00	7.58	9.44	5.74
6	1.00	7.39	9.19	5.58
7	1.00	7.12	8.84	5.37
8	1.00	6.11	7.59	4.61
9	1.00	1.31	1.65	1.00
10	1.00	3.96	4.91	2.98
11	1.00	2.47	3.09	1.88
12	1.00	7.32	9.13	5.55
13	1.00	3.74	4.68	2.83
14	1.00	6.19	7.74	4.71
15	1.00	2.07	2.56	1.55
16	1.00	1.34	1.66	1.01
17	1.00	11.55	14.33	8.69
18	1.00	12.69	15.83	9.63
19	1.00	11.61	14.42	8.73
20	1.00	0.86	1.07	0.64
21	1.00	13.82	17.19	10.42

Supplementary Table S5: Taxa sampled for phylogenetic inference. Localities and sampling coordinates are provided for sampling sites in Panama and Venezuela.

Scientific name	Locality	Sampling coordinates		Specimen ID
Ariopsis sp. nov. (*A. jimenezi*)	Pearl islands / Casaya island, Panama, PA	8°34′38.6″N	79°03′03.6″W	08E4
Ariopsis seemanni	Rio Estero Salado, Cocle, PA	8°10′30.3″N	80°29′35.1″W	08C8
Bagre bagre	Lago de Maracaibo / Isla de San Carlos, Zulia, VE	10°59′55.1″N	71°36′19.8″W	05A9
Bagre marinus	Gulf of Venezuela, Falcon, VE	11°14′15.3″N	70°30′53.1″W	05I5
Bagre panamensis	Rio Estero Salado, Cocle, PA	8°10′30.3″N	80°29′35.1″W	08C1
Bagre pinnimaculatus 1	Rio Estero Salado, Cocle, PA	8°10′30.3″N	80°29′35.1″W	08B7
Bagre pinnimaculatus 2	Gulf of Panama	8°48′56.6″N	79°22′50.9″W	01B6
Cathorops fuerthii	Rio Parita, Herrera, PA	8°01′13.7″N	80°27′11.2″W	08D5
Cathorops hypophthalmus	Rio Estero Salado, Cocle, PA	8°10′30.3″N	80°29′35.1″W	08C4
Cathorops nuchalis	Lago de Maracaibo / Puerto Concha, Zulia, VE	9°05′46.0″N	71°42′52.0″W	01G1
Cathorops tuyra	Puente del Rio Chagres,Colon, PA	9°11′34.7″N	79°39′09.4″W	08G2
Cathorops wayuu	Lago de Maracaibo / Guarico, Zulia, VE	10°43′52.0″N	71°31′40.2″W	05C7
Cathorops wayuu	Lago de Maracaibo / Isla de Toas, Zulia, VE	10°57′09.5″N	71°38′49.5″W	05G8
Notarius biffi	Rio San Pedro, Veraguas, PA	7°50′59.2″N	81°07′04.0″W	08A9
Notarius cookei	Rio Santa Maria, Cocle, PA	8°06′20.3″N	80°33′16.1″W	08G9
Notarius grandicassis	Gulf of Venezuela, Falcon, VE	11°14′15.3″N	70°30′53.1″W	05H9
Notarius kessleri	Rio San Pedro, Veraguas, PA	7°50′59.2″N	81°07′04.0″W	08A7
Notarius planiceps	Rio Estero Salado, Cocle, PA	8°10′30.3″N	80°29′35.1″W	08C2
Notarius quadriscutis	Clarines, Anzoategui, VE	10°03′46.8″N	65°11′05.2″W	03F1
Notarius dowii	Puerto Caimito, Panama, PA	8°52′18.9″N	79°42′33.0″W	08D9
Notarius dowii	Rio Santa Maria, Cocle, PA	8°06′20.3″N	80°33′16.1″W	08H1
Sciades herzbergii 1	Clarines, Anzoategui, VE	10°03′46.8″N	65°11′05.2″W	03C6
Sciades herzbergii 2	Gulf of Venezuela, Falcon, VE	11°14′15.3″N	70°30′53.1″W	04D9
Sciades parkeri	Ciudad Bolivar, Bolívar, VE	8°08′51.5″N	63°32′10.7″W	06B9
Sciades proops	Gulf of Venezuela, Falcon, VE	11°14′15.3″N	70°30′53.1″W	05I8
Sciades proops	Puerto La Cruz, Anzoategui, VE	10°12′58.6″N	64°38′39.2″W	06A9

PA, Panama; VE, Venezuela. Specimens of nominal species that are considered independent lineages in our phylogenetic analysis are marked with numbers 1,2.

Supplementary Table S6: Fossils of Neotropical sea catfishes used in phylogenetic analyses.

Species	Type	Formation	Locality	Epoch	Age (Ma)
Cathorops goeldii[1]	Skull	Pirabas Fm.	Atalaia Beach, Salinpolis Municipality, Para State, BR	Aquitanian[3]	23.0-20.4[4]
Notarius sp.[2]	Otolith				
Bagre protocaribbeanus[2]	Otolith				
Bagre protocaribbeanus[1]	Otolith	Cantaure Fm.	San José de Cocodite, VE	Burdigalian[5]	20.4-16.0[4]
Sciades dowii[6]	Skull	Urumaco Fm.	Urumaco, VE	Late Miocene[7]	11.6-5.3[4]
Sciades herzbergii[6]	Skull				
Bagre marinus[6]	Skull				
Notarius quadriscutis[6,8]	Skull				

BR, Brazil; VE, Venezuela.

[1]Aguilera et al. (2013); [2]Aguilera et al. (2014); [3]Aguilera et al. (2016); [4]Cohen et al. (2013);

[5]Carrillo-Briceño et al. (2016); [6]Aguilera and de Aguilera (2004); [7]Aguilera and Marceniuk (2012);

[8]Originally described as *Aspistor quadriscutis*; however, genus *Aspistor* is here considered synonymous with *Notarius*, following Betancur-R. and Acero P. (2004).

Supplementary Table S7: Node support, age estimates, and reconstructed ancestral geography for the species tree of Neotropical sea catfishes based on the MSC model. Lower and upper boundaries given for age estimates describe 95% HPD intervals. The ancestral geography of each node was reconstructed with two approaches: stochastic mapping of discrete characters (Huelsenbeck et al. 2003), implemented in the R package 'phytools' (Revell 2012) and the structured coalescent implementation in the BASTA package (De Maio et al. 2015b) for BEAST (Bouckaert et al. 2014). Node ids correspond to those given in Supplementary Figure S7.

					Geography (BPP)			
		Age estimates (Ma)			Stochastic mapping		BASTA	
Node	Node support (BPP)	Mean	Upper	Lower	Caribbean	TEP	Caribbean	TEP
1	1.00	29.04	31.35	26.86	0.81	0.19	0.77	0.23
2	1.00	22.24	24.06	20.68	0.99	0.01	0.99	0.01
3	0.92	21.33	23.00	20.40	1.00	0.00	0.99	0.01
4	1.00	19.06	20.94	17.45	0.89	0.11	0.87	0.13
5	1.00	5.44	6.63	4.39	0.11	0.89	0.17	0.83
6	1.00	6.74	7.90	5.74	1.00	0.00	0.99	0.01
7	1.00	5.98	6.98	5.30	1.00	0.00	0.99	0.01
8	0.62	6.43	7.50	5.48	1.00	0.00	0.99	0.01
9	0.79	6.06	7.08	4.98	1.00	0.00	0.98	0.02
10	1.00	5.91	6.73	5.30	1.00	0.00	0.99	0.01
11	1.00	1.64	2.20	1.04	1.00	0.00	0.99	0.01
12	1.00	20.86	21.86	20.40	1.00	0.00	1.00	0.00
13	1.00	20.62	21.28	20.40	1.00	0.00	1.00	0.00
14	1.00	10.93	12.29	9.60	0.77	0.23	0.72	0.28
15	1.00	9.70	11.05	8.50	0.81	0.19	0.77	0.23
16	0.98	8.89	10.17	7.67	0.89	0.11	0.84	0.16
17	1.00	7.11	9.01	5.31	0.97	0.03	0.93	0.07
18	1.00	1.66	2.30	1.08	0.02	0.98	0.03	0.97
19	1.00	21.28	22.78	20.40	0.99	0.01	0.98	0.02
20	1.00	11.61	13.23	10.21	0.70	0.30	0.70	0.30
21	1.00	9.63	10.99	8.30	0.65	0.35	0.65	0.35
22	0.54	11.29	12.75	9.86	0.70	0.30	0.71	0.29
23	1.00	10.17	11.59	8.90	0.55	0.45	0.59	0.41
24	1.00	1.72	2.36	1.15	0.02	0.98	0.03	0.97
25	1.00	8.33	11.23	5.32	0.90	0.10	0.87	0.13
26	1.00	24.65	28.95	20.41	0.87	0.13	0.81	0.19
27	1.00	6.90	8.12	5.85	0.20	0.80	0.22	0.78
28	1.00	5.68	6.74	4.63	0.12	0.88	0.17	0.83
29	1.00	2.58	3.37	1.87	0.36	0.64	0.36	0.64
30	1.00	0.46	0.74	0.22	1.00	0.00	1.00	0.00

References

Afonso Silva, A. C., N. Santos, H. A. Ogilvie, and C. Moritz. 2017. Validation and description of two new north-western Australian Rainbow skinks with multispecies coalescent methods and morphology. PeerJ 5:e3724.

Aguilera, O. and D. R. de Aguilera. 2004. Amphi-American Neogene sea catfishes (Siluriformes, Ariidae) from northern South America. Spec. Pap. Paleontol. 71:29–48.

Aguilera, O. and A. P. Marceniuk. 2012. *Aspistor verumquadriscutis*, a new fossil species of sea catfishes (Siluriformes; Ariidae) from the upper Miocene of Venezuela. Swiss J. Palaeontol. 131:265–274.

Aguilera, O., W. Schwarzhans, H. Moraes-Santos, and A. Nepomuceno. 2014. Before the flood: Miocene otoliths from eastern Amazon Pirabas Formation reveal a Caribbean-type fish fauna. J. South Am. Earth Sci. 56:422–446.

Aguilera, O. A., H. Moraes-Santos, S. Costa, F. Ohe, C. Jaramillo, and A. Nogueira. 2013. Ariid sea catfishes from the coeval Pirabas (Northeastern Brazil), Cantaure, Castillo (Northwestern Venezuela), and Castilletes (North Colombia) formations (early Miocene), with description of three new species. Swiss J. Palaeontol. 132:45–68.

Aguilera, O. A., W. Schwarzhans, and P. Béarez. 2016. Otoliths of the Sciaenidae from the Neogene of tropical America. Palaeo Ichthyologica 14:1–128.

Ahrens, C. W., M. A. Supple, N. C. Aitken, D. J. Cantrill, J. O. Borevitz, and E. A. James. 2017. Genomic diversity guides conservation strategies among rare terrestrial orchid species when taxonomy remains uncertain. Ann. Bot. 119:1267–1277.

Alter, S. E., J. Munshi-South, and M. L. J. Stiassny. 2017. Genomewide SNP data reveal cryptic phylogeographic structure and microallopatric divergence in a rapids-adapted clade of cichlids from the Congo River. Mol. Ecol. 26:1401–1419.

Anderson, B. M., K. R. Thiele, S. L. Krauss, and M. D. Barrett. 2017. Genotyping-by-sequencing in a species complex of Australian hummock grasses (*Triodia*): methodological insights and phylogenetic resolution. PLOS ONE 12:e0171053.

Battey, C. J. and J. Klicka. 2017. Cryptic speciation and gene flow in a migratory songbird species complex: Insights from the Red-Eyed Vireo (*Vireo olivaceus*). Mol. Phylogenet. Evol. 113:67–75.

Beddows, I., A. Reddy, T. Kloesges, and L. E. Rose. 2017. Population genomics in wild tomatoes - the interplay of divergence and admixture. Genome Biol. Evol. 9:3023–3038.

Bell, R. C., R. C. Drewes, and K. R. Zamudio. 2015. Reed frog diversification in the Gulf of Guinea: Overseas dispersal, the progression rule, and in situ speciation. Evolution 69:904–915.

Betancur-R., R. and A. Acero P. 2004. Description of *Notarius biffi* n. sp. and redescription of *N. insculptus* (Jordan and Gilbert) (Siluriformes: Ariidae) from the Eastern Pacific, with evidence of monophyly and limits of *Notarius*. Zootaxa 703:1–20.

Blanca, J., J. Montero-Pau, C. Sauvage, G. Bauchet, E. Illa, M. J. Díez, D. Francis, M. Causse, E. van der Knaap, and J. Cañizares. 2015. Genomic variation in tomato, from wild ancestors to contemporary breeding accessions. BMC Genomics 16:257.

Boucher, F. C., G. Casazza, P. Szövényi, and E. Conti. 2016. Sequence capture using RAD probes clarifies phylogenetic relationships and species boundaries in *Primula* sect. *Auricula*. Mol. Phylogenet. Evol. 104:60–72.

Bouckaert, R. R., J. Heled, D. Kühnert, T. Vaughan, C.-H. Wu, D. Xie, M. A. Suchard, A. Rambaut, and A. J. Drummond. 2014. BEAST 2: a software platform for Bayesian evolutionary analysis. PLOS Comput. Biol. 10:e1003537.

Bryant, D., R. R. Bouckaert, J. Felsenstein, N. A. Rosenberg, and A. RoyChoudhury. 2012. Inferring species trees directly from biallelic genetic markers: bypassing gene trees in a full coalescent analysis. Mol. Biol. Evol. 29:1917–1932.

Bryson, R. W., Jr., W. E. Savary, A. J. Zellmer, R. B. Bury, and J. E. McCormack. 2016. Genomic data reveal ancient microendemism in forest scorpions across the California Floristic Province. Mol. Ecol. 25:3731–3751.

Burns, M. and N. Tsurusaki. 2016. Male reproductive morphology across latitudinal clines and under long-term female sex-ratio bias. Integr. Comp. Biol. 56:715–727.

Card, D. C., D. R. Schield, R. H. Adams, A. B. Corbin, B. W. Perry, A. L. Andrew, G. I. M. Pasquesi, E. N. Smith, T. Jezkova, S. M. Boback, W. Booth, and T. A. Castoe. 2016. Phylogeographic and population genetic analyses reveal multiple species of *Boa* and independent origins of insular dwarfism. Mol. Phylogenet. Evol. 102:104–116.

Carrillo-Briceño, J. D., O. A. Aguilera, C. De Gracia, G. Aguirre-Fernández, R. Kindlimann, and M. R. Sánchez-Villagra. 2016. An Early Neogene Elasmobranch fauna from the southern Caribbean (Western Venezuela). Palaeontol. Electron. 19.2.27A:1–32.

Chan, K. O., A. M. Alexander, L. L. Grismer, Y.-C. Su, J. L. Grismer, E. S. H. Quah, and R. M. Brown. 2017. Species delimitation with gene flow: A methodological comparison and population genomics approach to elucidate cryptic species boundaries in Malaysian Torrent Frogs. Mol. Ecol. 26:5435–5450.

Chifman, J. and L. Kubatko. 2014. Quartet inference from SNP data under the coalescent model. Bioinformatics 30:3317–3324.

Clucas, G. V., J. L. Younger, D. Kao, A. D. Rogers, J. Handley, G. D. Miller, P. Jouventin, P. Nolan, K. Gharbi, K. J. Miller, and T. Hart. 2016. Dispersal in the sub-Antarctic: king penguins show remarkably little population genetic differentiation across their range. BMC Evol. Biol. 16:211.

Cohen, K., S. Finney, P. Gibbard, and J.-X. Fan. 2013. The ICS International Chronostratigraphic Chart. Episodes 36: 199-204. Available from `http://www.stratigraphy.org/ICSchart/ChronostratChart2015-01.pdf`.

Cooper, E. A. and J. A. C. Uy. 2017. Genomic evidence for convergent evolution of a key trait underlying divergence in island birds. Mol. Ecol. 26:3760–3774.

DaCosta, J. M. and M. D. Sorenson. 2016. ddRAD-seq phylogenetics based on nucleotide, indel, and presence–absence polymorphisms: Analyses of two avian genera with contrasting histories. Mol. Phylogenet. Evol. 94:122–135.

De Maio, N., D. Schrempf, and C. Kosiol. 2015a. PoMo: An allele frequency-based approach for species tree estimation. Syst. Biol. 64:1018–1031.

De Maio, N., C.-H. Wu, K. M. O'Reilly, and D. Wilson. 2015b. New routes to phylogeography: A Bayesian structured coalescent approximation. PLOS Genet. 11:e1005421.

Demos, T. C., J. C. Kerbis Peterhans, T. A. Joseph, J. D. Robinson, B. Agwanda, and M. J. Hickerson. 2015. Comparative population genomics of African montane forest mammals support population persistence across a climatic gradient and Quaternary climatic cycles. PLOS ONE 10:e0131800.

Drummond, A. J., G. K. Nicholls, A. G. Rodrigo, and W. Solomon. 2002. Estimating mutation parameters, population history and genealogy simultaneously from temporally spaced sequence data. Genetics 161:1307–1320.

Dupuis, J. R., B. M. T. Brunet, H. M. Bird, L. M. Lumley, G. Fagua, B. Boyle, R. Levesque, M. Cusson, J. A. Powell, and F. A. H. Sperling. 2017. Genome-wide SNPs resolve phylogenetic relationships in the North American spruce budworm (*Choristoneura fumiferana*) species complex. Mol. Phylogenet. Evol. 111:158–168.

Foote, A. D. and P. A. Morin. 2016. Genome-wide SNP data suggest complex ancestry of sympatric North Pacific killer whale ecotypes. Heredity 117:316–325.

Ford, A. G. P., K. K. Dasmahapatra, L. Rüber, K. Gharbi, T. Cezard, and J. J. Day. 2015. High levels of interspecific gene flow in an endemic cichlid fish adaptive radiation from an extreme lake environment. Mol. Ecol. 24:3421–3440.

Fraser, C. I., A. Mcgaughran, A. Chuah, and J. M. Waters. 2016. The importance of replicating genomic analyses to verify phylogenetic signal for recently evolved lineages. Mol. Ecol. 25:3683–3695.

Giarla, T. C. and J. A. Esselstyn. 2015. The challenges of resolving a rapid, recent radiation: empirical and simulated phylogenomics of Philippine shrews. Syst. Biol. 64:727–740.

Gohli, J., E. H. Leder, E. Garcia-del Rey, L. E. Johannessen, A. Johnsen, T. Laskemoen, M. Popp, and J. T. Lifjeld. 2014. The evolutionary history of Afrocanarian blue tits inferred from genomewide SNPs. Mol. Ecol. 24:180–191.

Gottscho, A. D., D. A. Wood, A. G. Vandergast, J. Lemos-Espinal, J. Gatesy, and T. W. Reeder. 2017. Lineage diversification of fringe-toed lizards (Phrynosomatidae: *Uma notata* complex) in the Colorado Desert: Delimiting species in the presence of gene flow. Mol. Phylogenet. Evol. 106:103–117.

Gratton, P., E. Trucchi, A. Trasatti, G. Riccarducci, S. Marta, G. Allegrucci, D. Cesaroni, and V. Sbordoni. 2016. Testing classical species properties with contemporary data: how "bad species" in the brassy ringlets (*Erebia tyndarus* complex, Lepidoptera) turned good. Syst. Biol. 65:292–303.

Hamlin, J. A. P. and M. L. Arnold. 2014. Determining population structure and hybridization for two iris species. Ecol. Evol. 4:743–755.

Harrington, S. M., B. D. Hollingsworth, T. E. Higham, and T. W. Reeder. 2017. Pleistocene climatic fluctuations drive isolation and secondary contact in the red diamond rattlesnake (*Crotalus ruber*) in Baja California. J. Biogeogr. 55:369.

Harris, R. B., P. Alström, A. Ödeen, and A. D. Leaché. 2017. Discordance between genomic divergence and phenotypic variation in a rapidly evolving avian genus (*Motacilla*). arXiv preprint, arXiv:170703864:1–26.

Harvey, M. G. and R. T. Brumfield. 2015. Genomic variation in a widespread Neotropical bird (*Xenops minutus*) reveals divergence, population expansion, and gene flow. Mol. Phylogenet. Evol. 83:305–316.

Herrera, S. and T. M. Shank. 2016. RAD sequencing enables unprecedented phylogenetic resolution and objective species delimitation in recalcitrant divergent taxa. Mol. Phylogenet. Evol. 100:70–79.

Huelsenbeck, J. P., R. Nielsen, and J. P. Bollback. 2003. Stochastic mapping of morphological characters. Syst. Biol. 52:131–158.

Hulsey, C. D., J. Zheng, B. C. Faircloth, A. Meyer, and M. E. Alfaro. 2017. Phylogenomic analysis of Lake Malawi cichlid fishes: Further evidence that the three-stage model of diversification does not fit. Mol. Phylogenet. Evol. 114:40–48.

Johansson, F., P. Halvarsson, D. J. Mikolajewski, and J. Höglund. 2017. Phylogeography and larval spine length of the dragonfly *Leucorhinia dubia* in Europe. PLOS ONE 12:e0184596.

Kautt, A. F., G. Machado-Schiaffino, and A. Meyer. 2016. Multispecies outcomes of sympatric speciation after admixture with the source population in two radiations of Nicaraguan crater lake cichlids. PLOS Genet. 12:e1006157.

Kordbacheh, A., G. Garbalena, and E. J. Walsh. 2017. Population structure and cryptic species in the cosmopolitan rotifer *Euchlanis dilatata*. Zoological Journal of the Linnean Society 181:757–777.

Lambert, S. M., A. J. Geneva, D. Luke Mahler, and R. E. Glor. 2013. Using genomic data to revisit an early example of reproductive character displacement in Haitian *Anolis* lizards. Mol. Ecol. 22:3981–3995.

Leaché, A. D., M. K. Fujita, V. N. Minin, and R. R. Bouckaert. 2014. Species delimitation using genome-wide SNP data. Syst. Biol. 63:534–542.

Li, C., S. Corrigan, L. Yang, N. Straube, M. Harris, M. Hofreiter, W. T. White, and G. J. P. Naylor. 2015. DNA capture reveals transoceanic gene flow in endangered river sharks. Proc. Natl. Acad. Sci. USA 112:13302–13307.

Lischer, H. E. L., L. Excoffier, and G. Heckel. 2014. Ignoring heterozygous sites biases phylogenomic estimates of divergence times: implications for the evolutionary history of *Microtus* voles. Mol. Biol. Evol. 31:817–831.

Lozier, J. D., J. M. Jackson, M. E. Dillon, and J. P. Strange. 2016. Population genomics of divergence among extreme and intermediate color forms in a polymorphic insect. Ecol. Evol. 6:1075–1091.

MacGuigan, D. J., A. J. Geneva, and R. E. Glor. 2017. A genomic assessment of species boundaries and hybridization in a group of highly polymorphic anoles (*distichus* species complex). Ecol. Evol. 7:3657–3671.

MacLeod, A., A. Rodríguez, M. Vences, P. Orozco-terWengel, C. García, F. Trillmich, G. Gentile, A. Caccone, G. Quezada, and S. Steinfartz. 2015. Hybridization masks speciation in the evolutionary history of the Galápagos marine iguana. Proc. R. Soc. B 282:20150425.

Malinsky, M., H. Svardal, A. M. Tyers, E. A. Miska, M. J. Genner, G. F. Turner, and R. Durbin. 2017. Whole genome sequences of Malawi cichlids reveal multiple radiations interconnected by gene flow. bioRxiv preprint, doi: 101101/143859.

Manthey, J. D., L. C. Campillo, K. J. Burns, and R. G. Moyle. 2016. Comparison of target-capture and restriction-site associated DNA sequencing for phylogenomics: a test in cardinalid tanagers (Aves, genus: *Piranga*). Syst. Biol. 65:640–650.

Manthey, J. D., J. Klicka, and G. M. Spellman. 2015. Chromosomal patterns of diversity and differentiation in creepers: a next-gen phylogeographic investigation of *Certhia americana*. Heredity 115:165–172.

Mason, N. A. and S. A. Taylor. 2015. Differentially expressed genes match bill morphology and plumage despite largely undifferentiated genomes in a Holarctic songbird. Mol. Ecol. 24:3009–3025.

McCormack, J. E., W. L. E. Tsai, and B. C. Faircloth. 2015. Sequence capture of ultraconserved elements from bird museum specimens. Mol. Ecol. Resour. 16:1189–1203.

Meier, J. I., D. A. Marques, S. Mwaiko, C. E. Wagner, L. Excoffier, and O. Seehausen. 2017. Ancient hybridization fuels rapid cichlid fish adaptive radiations. Nat. Commun. 8:1–11.

Meik, J. M., J. W. Streicher, A. M. Lawing, O. Flores-Villela, and M. K. Fujita. 2015. Limitations of climatic data for inferring species boundaries: insights from speckled rattlesnakes. PLOS ONE 10:e0131435.

Morin, P. A., K. M. Parsons, F. I. Archer, M. C. Ávila-Arcos, L. G. Barrett-Lennard, L. Dalla Rosa, S. Duchêne, J. W. Durban, G. M. Ellis, S. H. Ferguson, J. K. Ford, M. J. Ford, C. Garilao, M. T. P. Gilbert, K. Kaschner, C. O. Matkin, S. D. Petersen, K. M. Robertson, I. N. Visser, P. R. Wade, S. Y. W. Ho, and A. D. Foote. 2015. Geographic and temporal dynamics of a global radiation and diversification in the killer whale. Mol. Ecol. 24:3964–3979.

Mrinalini, R. S. Thorpe, S. Creer, D. Lallias, L. Dawnay, B. L. Stuart, and A. Malhotra. 2015. Convergence of multiple markers and analysis methods defines the genetic distinctiveness of cryptic pitvipers. Mol. Phylogenet. Evol. 92:266–279.

Nater, A., R. Burri, T. Kawakami, L. Smeds, and H. Ellegren. 2015. Resolving evolutionary relationships in closely related species with whole-genome sequencing data. Syst. Biol. 64:1000–1017.

Ng, N. S. R., P. R. Wilton, D. M. Prawiradilaga, Y. C. Tay, M. Indrawan, K. M. Garg, and F. E. Rheindt. 2017. The effects of Pleistocene climate change on biotic differentiation in a montane songbird clade from Wallacea. Mol. Phylogenet. Evol. 114:353–366.

Nicotra, A. B., C. Chong, J. G. Bragg, C. R. Ong, N. C. Aitken, A. Chuah, B. Lepschi, and J. O. Borevitz. 2016. Population and phylogenomic decomposition via genotyping-by-sequencing in Australian *Pelargonium*. Mol. Ecol. 25:2000–2014.

Nieto-Montes de Oca, A., A. J. Barley, R. N. Meza-Lázaro, U. O. García-Vázquez, J. G. Zamora-Abrego, R. C. Thomson, and A. D. Leaché. 2017. Phylogenomics and species delimitation in the knob-scaled lizards of the genus *Xenosaurus* (Squamata: Xenosauridae) using ddRADseq data reveal a substantial underestimation of diversity. Mol. Phylogenet. Evol. 106:241–253.

Ogilvie, H. A., J. Heled, D. Xie, and A. J. Drummond. 2016. Computational performance and statistical accuracy of *BEAST and comparisons with other methods. Syst. Biol. 65:381–396.

Olšavská, K., M. Slovák, K. Marhold, and E. Štubňová. 2016. On the origins of Balkan endemics: the complex evolutionary history of the *Cyanus napulifer* group (Asteraceae). Ann. Bot. 118:1071–1088.

Oswald, J. A., M. G. Harvey, R. C. Remsen, D. U. Foxworth, S. W. Cardiff, D. L. Dittmann, L. C. Megna, M. D. Carling, and R. T. Brumfield. 2016. Willet be one species or two? A genomic view of the evolutionary history of *Tringa semipalmata*. The Auk 133:593–614.

Papadopoulou, A. and L. L. Knowles. 2017. Linking micro- and macroevolutionary perspectives to evaluate the role of Quaternary sea-level oscillations in island diversification. Evolution 71:2901–2917.

Paun, O., B. Turner, E. Trucchi, J. Munzinger, M. W. Chase, and R. Samuel. 2016. Processes driving the adaptive radiation of a tropical tree (*Diospyros*, Ebenaceae) in New Caledonia, a biodiversity hotspot. Syst. Biol. 65:212–227.

Portik, D. M., A. D. Leaché, D. Rivera, M. F. Barej, M. Burger, M. Hirschfeld, M.-O. Rödel, D. C. Blackburn, and M. K. Fujita. 2017. Evaluating mechanisms of diversification in a Guineo-Congolian tropical forest frog using demographic model selection. Mol. Ecol. 26:5245–5263.

Potter, S., J. G. Bragg, B. M. Peter, K. Bi, and C. Moritz. 2016. Phylogenomics at the tips: inferring lineages and their demographic history in a tropical lizard, *Carlia amax*. Mol. Ecol. 25:1367–1380.

Razkin, O., G. Sonet, K. Breugelmans, M. J. Madeira, B. J. Gómez-Moliner, and T. Backeljau. 2016. Species limits, interspecific hybridization and phylogeny in the cryptic land snail complex *Pyramidula*: The power of RADseq data. Mol. Phylogenet. Evol. 101:267–278.

Revell, L. J. 2012. phytools: an R package for phylogenetic comparative biology (and other things). Method Ecol. Evol. 3:217–223.

Rheindt, F. E., M. K. Fujita, P. R. Wilton, and S. V. Edwards. 2014. Introgression and phenotypic assimilation in *Zimmerius* flycatchers (Tyrannidae): population genetic and phylogenetic inferences from genome-wide SNPs. Syst. Biol. 63:134–152.

Rittmeyer, E. N. and C. C. Austin. 2015. Combined next-generation sequencing and morphology reveal fine-scale speciation in Crocodile Skinks (Squamata: Scincidae: *Tribolonotus*). Mol. Ecol. 24:466–483.

Rodríguez, A., J. D. Burgon, M. Lyra, I. Irisarri, D. Baurain, L. Blaustein, B. Göçmen, S. Künzel, B. K. Mable, A. W. Nolte, M. Veith, S. Steinfartz, K. R. Elmer, H. Philippe, and M. Vences. 2017. Inferring the shallow phylogeny of true salamanders (*Salamandra*) by multiple phylogenomic approaches. Mol. Phylogenet. Evol. 115:16–26.

Schield, D. R., R. H. Adams, D. C. Card, B. W. Perry, G. M. Pasquesi, T. Jezkova, D. M. Portik, A. L. Andrew, C. L. Spencer, E. E. Sanchez, M. K. Fujita, S. P. Mackessy, and T. A. Castoe. 2017. Insight into the roles of selection in speciation from genomic patterns of divergence and introgression in secondary contact in venomous rattlesnakes. Ecol. Evol. 7:3951–3966.

Schmidt-Lebuhn, A. N., N. C. Aitken, and A. Chuah. 2017. Species trees from consensus single nucleotide polymorphism (SNP) data: Testing phylogenetic approaches with simulated and empirical data. Mol. Phylogenet. Evol. 116:192–201.

Sovic, M. G., A. C. Fries, and H. L. Gibbs. 2016. Origin of a cryptic lineage in a threatened reptile through isolation and historical hybridization. Heredity 117:358–366.

Stange, M., G. Aguirre-Fernández, R. G. Cooke, T. Barros, W. Salzburger, and M. R. Sánchez-Villagra. 2016. Evolution of opercle bone shape along a macrohabitat gradient: species identification using mtDNA and geometric morphometric analyses in neotropical sea catfishes (Ariidae). Ecol. Evol. 6:5817–5830.

Stervander, M., P. Alström, U. Olsson, U. Ottosson, B. Hansson, and S. Bensch. 2016. Multiple instances of paraphyletic species and cryptic taxa revealed by mitochondrial and nuclear RAD data for *Calandrella* larks (Aves: Alaudidae). Mol. Phylogenet. Evol. 102:233–245.

Stervander, M., J. C. Illera, L. Kvist, P. Barbosa, N. P. Keehnen, P. Pruisscher, S. Bensch, and B. Hansson. 2015. Disentangling the complex evolutionary history of the Western Palearctic blue tits (*Cyanistes* spp.) - phylogenomic analyses suggest radiation by multiple colonization events and subsequent isolation. Mol. Ecol. 24:2477–2494.

Stetter, M. G. and K. J. Schmid. 2017. Analysis of phylogenetic relationships and genome size evolution of the *Amaranthus* genus using GBS indicates the ancestors of an ancient crop. Mol. Phylogenet. Evol. 109:80–92.

Streicher, J. W., T. J. Devitt, C. S. Goldberg, J. H. Malone, H. Blackmon, and M. K. Fujita. 2014. Diversification and asymmetrical gene flow across time and space: lineage sorting and hybridization in polytypic barking frogs. Mol. Ecol. 23:3273–3291.

Takahashi, H., T. Kondou, N. Takeshita, T.-H. Hsu, and M. Nishida. 2016. Evolutionary process of iwame, a markless form of the red-spotted masu salmon *Oncorhynchus masou ishikawae*, in the Ono River, Kyushu. Ichthyol. Res. 63:132–144.

Takahashi, H., N. Takeshita, H. Tanoue, S. Ueda, H. Takeshima, T. Komatsu, I. Kinoshita, and M. Nishida. 2015. Severely depleted genetic diversity and population structure of a large predatory marine fish (*Lates japonicus*) endemic to Japan. Conserv. Genet. 16:1155–1165.

Tremetsberger, K., M. Á. Ortiz, A. Terrab, F. Balao, R. Casimiro-Soriguer, M. Talavera, and S. Talavera. 2016. Phylogeography above the species level for perennial species in a composite genus. AoB PLANTS 8:plv142.

Wagner, F., S. Härtl, R. Vogt, and C. Oberprieler. 2017. "Fix Me Another Marguerite!": Species delimitation in a group of intensively hybridizing lineages of ox-eye daisies (*Leucanthemum* Mill., Compositae-Anthemideae). Mol. Ecol. 26:4260–4283.

Winger, B. M., P. A. Hosner, G. A. Bravo, A. M. Cuervo, N. Aristizábal, L. E. Cueto, and J. M. Bates. 2015. Inferring speciation history in the Andes with reduced-representation sequence data: an example in the bay-backed antpittas (Aves; Grallariidae; *Grallaria hypoleuca* s. l.). Mol. Ecol. 24:6256–6277.

Yoder, A. D., C. R. Campbell, M. B. Blanco, M. dos Reis, J. U. Ganzhorn, S. M. Goodman, K. E. Hunnicutt, P. A. Larsen, P. M. Kappeler, R. M. Rasoloarison, J. M. Ralison, D. L. Swofford, and D. W. Weisrock. 2016. Geogenetic patterns in mouse lemurs (genus *Microcebus*) reveal the ghosts of Madagascar's forests past. Proc. Natl. Acad. Sci. USA 113:8049–8056.

Younger, J. L., G. V. Clucas, D. Kao, A. D. Rogers, K. Gharbi, T. Hart, and K. J. Miller. 2017. The challenges of detecting subtle population structure and its importance for the conservation of emperor penguins. Mol. Ecol. 26:3883–3897.

Yuan, H., J. Jiang, F. A. Jiménez, E. P. Hoberg, J. A. Cook, K. E. Galbreath, and C. Li. 2016. Target gene enrichment in the cyclophyllidean cestodes, the most diverse group of tapeworms. Mol. Ecol. Resour. 16:1095–1106.

Zarza, E., B. C. Faircloth, W. L. E. Tsai, R. W. Bryson, Jr., J. Klicka, and J. E. McCormack. 2016. Hidden histories of gene flow in highland birds revealed with genomic markers. Mol. Ecol. 25:5144–5157.